Early extra-uterine exposure alters regional cerebellar growth in infants born preterm

Marie Brossard-Racine[a,b,d], Robert McCarter[c], Jonathan Murnick[e], Tinkleman L.[d], Gilbert Vezina[e], Catherine Limperopoulos[d,e,*]

[a] McGill University Health Centre Research Institute, Division of Pediatric Neonatology, Montreal, PQ, Canada
[b] School of Physical and Occupational Therapy, McGill University, Montreal, PQ, Canada
[c] Center for Translational Science, Children's National Health System, Washington, D.C., United States
[d] Center for the Developing Brain, Children's National Health System, Washington, D.C., United States
[e] Division of Diagnostic Imaging and Radiology, Children's National Health System, Washington, D.C., United States

ABSTRACT

Objectives: To compare third trimester global and regional cerebellar volumetric growth at two time-points between very preterm (PT) infants and healthy gestational age-matched fetuses in the PT period and at term equivalent age (TEA).

Study design: Using a prospective study design, high resolution anatomic magnetic resonance images (MRI) were acquired in PT infants (gestational age at birth < 32 weeks; birthweight < 1500 g) without cerebellar injury and healthy full-term controls. PT infants completed two MRIs, one as soon as medically stable and the other around TEA. Controls also completed two MRIs, one in utero (i.e. fetal MRI) and a postnatal MRI shortly after birth. The cerebellum of each participant was parcellated into 5 regions: left and right hemispheres, the anterior, neo and posterior vermis. Evidence of differences in regional volumes between term and pre-term infants matched for gestational age (GA) at the time of the first MRI were assessed using multiple linear regression.

Results: we studied 76 subjects: 38 PT infants were matched to 38 healthy fetuses. At MRI-1, PT infants demonstrated decreased cerebellar hemispheric volumes and increased anterior, neo- and posterior vermian regional volumes when compared to healthy fetuses. At TEA, PT infants demonstrated a persistent increase in anterior, neo- and posterior vermian regional volumes but no longer showed reductions in cerebellar hemispheric volume. Only the neovermis volume demonstrated a significant negative association with birthweight, male gender and supratentorial injury.

Conclusions: In the absence of demonstrable cerebellar parenchymal injury evident on conventional MRI, PT birth is associated with cerebellar growth alterations that are regionally- and temporally-specific.

1. Background

During the third trimester of pregnancy, the cerebellum undergoes its most rapid period of growth and development that is unparalleled by any other region of the brain, rendering it vulnerable to a host of potential insults including extra-uterine exposures unique to the premature infant (Limperopoulos et al., 2005a; Volpe, 2009). Available evidence suggests that premature exposure to the extra-uterine environment disrupts the cerebellum's programmed developmental course and increases the risk for cerebellar injury (Limperopoulos et al., 2005b). Preterm cerebellar hemorrhagic injury has been shown to stunt

cerebellar growth and adversely affect long-term neurodevelopment (Brossard-Racine et al., 2015; Limperopoulos et al., 2007). However, even in the absence of direct cerebellar parenchymal injury, cerebellar growth impairment is increasingly detected in survivors of prematurity (de Kieviet et al., 2012; Brossard-Racine et al., 2017a). These cerebellar insults have been associated with adverse motor, cognitive and behavioral outcomes commonly reported in the preterm population (Brossard-Racine et al., 2015). Because of the retrospective or cross-sectional nature of prior work, available studies have lacked sensitivity for cerebellar growth impairment, as well as the lack of truly normative fetal MRI cerebellar data for third trimester cerebellar development, the

---

underlying mechanisms and consequences of prematurity-related cerebellar growth remain poorly understood.

Our group recently published the first prospective third trimester study comparing ex-utero preterm (PT) infants and healthy in utero fetuses (Bouyssi-Kobar et al., 2016). In this cross-sectional study, we reported reduced cerebellar growth in PT infants between 27 and 39 weeks of gestation versus our normative fetal cohort. During fetal development, the cerebellar vermis develops and differentiates later and independently of the cerebellar hemispheres (Cho et al., 2011). However, our previous study did not evaluate longitudinal change or regional cerebellar differences which could help elucidate selective vulnerability for later functional deficits. Therefore, in the current study, we sought to characterize the temporal and regional topographic impairments of cerebellar growth in infants born prematurely. Specifically, our aim is to compare change in third trimester global and regional cerebellar volumetric growth between two time-points in very PT infants and healthy gestational age-matched fetuses in the PT period and at term equivalent age.

2. Methods

2.1. Subjects

As part of a prospective longitudinal study that begun in June 2015, we evaluated PT infants born ≤ 32 weeks of gestation and of ≤ 1500 g birth weight admitted to the NICU of the Children's National Health System (CNHS). Infants with congenital malformations or dysmorphic features suggestive of a genetic syndrome, confirmed metabolic disorder, central nervous system infection or chromosomal abnormality were excluded. Enrolled PT infants completed two magnetic resonance imaging (MRI), one as soon as medically stable (i.e. MRI-1) and the other around term equivalent age (TEA) (i.e. MRI-2).

A control group was used from a parallel study evaluating serial brain development in-utero and postnatally in healthy full term born infants (≥ 37 weeks of gestation) from healthy pregnant volunteers (Brossard-Racine et al., 2014). Controls with multiple pregnancies, fetal ultrasound/neonatal brain MRI abnormalities, congenital infection, documented chromosomal abnormalities and/or multi-organ dysmorphic conditions were excluded. Controls also completed two MRIs, one in utero (i.e. fetal MRI) and a postnatal MRI shortly after birth. Controls included in this study were matched to PT infants based on gestational age at MRI-1.

Prenatal, perinatal, and postnatal information for all enrolled subjects was collected through medical records abstractions and parental questionnaires and included the following variables: gender, GA at birth, birthweight, Apgar at 5 min, intubation at birth, bronchopulmonary dysplasia, patent ductus arteriosus ligation, necrotizing enterocolitis surgery, clinical infection as determined by a positive culture or 7 days or more of antibiotic treatment, postnatal steroid treatment, hypotension requiring vasoactive medication or use of sedation during the first five days of life, number of days on ventilator, number of days on supplementary oxygen, number of days in the NICU and brain injury. Written informed consent was obtained from the parents for every study participant, and the study was approved by CNHS IRB.

2.2. Preterm MRI acquisitions

PT infants underwent their first MRI-1 as soon as they were deemed medically stable by the attending neonatologist using a MRI compatible incubator (LMT Medical System GmbH, Luebeck, Germany). The PT MRI was performed on a 1.5 Tesla MRI scanner (Discovery MR450, General Electric Medical, Systems-Waukesha, WI) with a 1-channel receiver head coil. Two millimeter sagittal, coronal and axial single-shot fast spin echo (SSFSE) T2 weighted sequences (TR = 1100 ms, TE = 160 ms, FOV = 12, acquisition matrix = $192 \times 128 \text{ mm}^3$) were

acquired as well as susceptibility-weighted imaging (SWAN) (TR = 92.6 ms, TE = 48.6 ms, FOV = 16, acquisition matrix = $320 \times 224 \text{ mm}^3$). PT infants with cerebellar parenchymal injury on MRI-1 were subsequently excluded from this study.

2.3. Fetal MRI acquisitions

Healthy pregnant controls completed their fetal MRI-1 a 1.5 Tesla General Electric scanner using an 8-channel phased-array coil. Similar two millimeter sagittal, coronal and axial T2 SSFSE sequences were acquired (Brossard-Racine et al., 2014). No contrast or sedation was used for any of the fetal MRIs. All studies were reviewed for the presence of developmental malformations, maturation status and acquired abnormalities by an experienced fetal neuroradiologist (GV).

2.4. Neonatal MRI acquisition

All PT infants at TEA and neonates controls completed MRI-2 on the same 3 Tesla MRI scanner (Discovery MR750, General Electric Medical, Systems-Waukesha, WI) with an 8-channel receiver head coil. The MRI acquisition protocol included one millimeter 3-dimensional anatomical T2 images (T2 3D-Cube, TR = 2500 ms, TE = 62.7 ms, FOV = 16, acquisition matrix = $160 \times 160 \text{ mm}^3$), T1 images (T1 3D-SPGR, TR = 6.7 ms, TE = 4.1 ms, FOV = 16, acquisition matrix = $160 \times 160 \text{ mm}^3$), and SWAN (TR = 68 ms, TE = 25 ms, FOV = 16, acquisition matrix = $320 \times 224 \text{ mm}^3$). Unless clinically indicated for the PT infants, no sedation or intravenous injection of gadolinium-based contrast agents were used during the neonatal MRIs. Each infant's brain MRI study was reviewed by an experienced pediatric neuroradiologist (JM & GV). For PT infants at TEA, an overall score (from 0 to 40) for MRI abnormalities was given using Kidokoro et al.'s scoring system (Kidokoro et al., 2013), a specific scale developed for preterm infants evaluated at TEA. Using Kidokoro's scoring system, we created a supratentorial injury (SPI) score, which is derived from the sum of the subscores given to the cerebral white matter, cerebral cortical grey matter and cerebral deep grey mater. We used this SPI score in an attempt to isolate the effect of SPI on cerebellar volume as opposed to using the scale's total injury score which also includes 2-dimensional measurements of the cerebellum. Lastly, germinal matrix hemorrhage and intraventricular hemorrhage (GMH-IVH) were graded according to Papile's grading system (Barkovich, 2005).

2.5. 3-D volumetric analyses of the cerebellum

All anatomical images underwent visual quality inspection and only motion and artifact free images were selected for this study. For images acquired on the 1.5 T scanner (i.e. MRI-1, PT or fetal MRI), the 2-dimensional SSFSE images acquired were corrected for intensity non-homogeneity and 3-dimensional reconstructions of the brain were performed (Gholipour et al., 2011; Tustison et al., 2010). For the anatomical images acquired on the 3 T scanner (i.e. MRI-2), the T2 3D-Cube and T1 3D-SPGR were co-registered together. Thereafter, manual parcellation of the cerebellum was performed for each pair of anatomical images for each subject using ITK-SNAP software by two independent evaluators (MBR & LK) (Yushkevich et al., 2006). The cerebellum was parcellated into 5 regions: left and right hemispheres, the anterior (lobules I/II, III, IV and V), neo (lobules VI, VIIA and VIIB) and posterior vermis (VIIIA, VIIIB, IX and X) (Fig. 1) based on anatomic landmarks as outlined by Bogovic et al.'s (2013) lobular parcellation protocol (Bogovic et al., 2013). Due to the decreased MR image resolution, we could not consistently identify the primary fissure on the cerebellar hemispheres and therefore could not reliably parcellate the anterior and posterior hemispheres. Together the sum of these measures formed the total cerebellar volume (in centimeters cube). The total brain volume (TBV) was also extracted from a complete brain mask obtained using the Brain ExtractionTool (Smith, 2002).
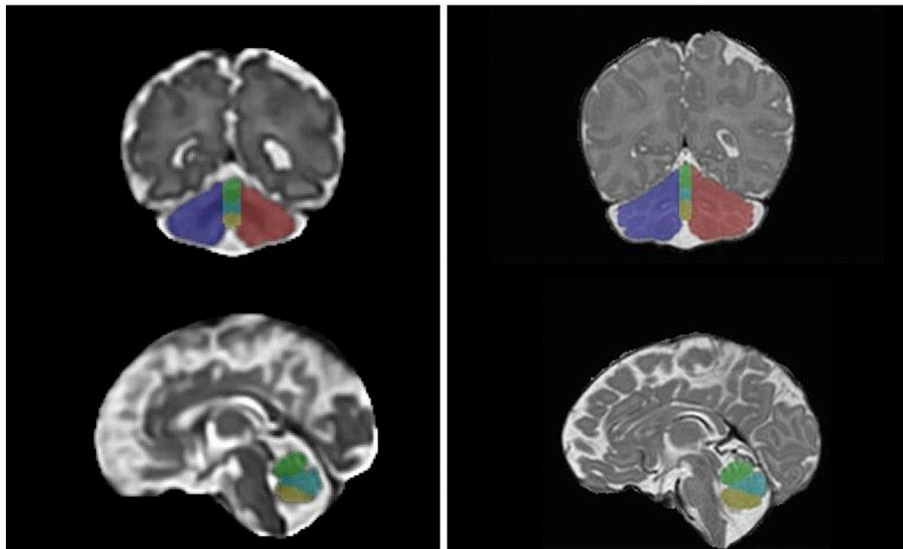
Fig. 1. Parcellation of the cerebellum on coronal (top) and sagittal (bottom) T2 images in a healthy fetus at 25 2/7 weeks GA (left) and neonate 40 5/7 weeks GA (right). Color legend: Blue = left hemisphere, green = anterior vermis, cyan = neovermis, yellow = posterior vermis, red = right hemisphere.

Five fetuses and five neonates were analyzed twice by each evaluator following a 24-h interval to assess intra-rater reliability. Intraclass coefficient for intra-rater reliability ranged between 0.90 and 0.99. Additionally, inter-rater reliability was assessed between the two evaluators for these same ten subjects and intra-class coefficient ranged between 0.92 and 0.99.

2.6. Statistical analyses

We developed multiple linear regression models in Stata 14 (StataCorp, 2015) to evaluate evidence of differences in regional volumes between term and pre-term infants matched for gestational age (GA) at the time of the first MRI. All models evaluated the need for interactions between cerebellar regions and term-PT to account for differential effects per region and controlled for GA at MRI to remove any differences not equalized by the pairings. All models treated term-PT pairs as data clusters to adjust standard error estimates for the correlation between paired subjects. Initial models focused on difference at MRI-1 controlling for GA at MRI-1. The second set of models focused on results of MRI-2 on the same paired infants initially controlling for each respective cerebellar regional volume at MRI-1 and GA at MRI-2. Models were thereafter repeated additionally controlling for total brain volume. We estimated the adjusted volume for term and PT infants in each brain region and performed linear contrasts to determine where term-PT differences in volumes occurred after detecting overall evidence of regional differences.

Subsequently, in regions showing volume differences at MRI-2, we used the model that best predicted regional volume differences between term and PT infants to evaluate the relationship of potential risk factors with volumetric differences in the PT infants at MRI-2. This was accomplished by adding each candidate risk factor to the best predictive model for each region using only the PT group for which risk factor data was available. If more than one risk factor was identified per site we then combined these into multiple risk factor models in an attempt to improve prediction of volumetric differences.

3. Results

3.1. Subject characteristics

A total of 38 PT infants were matched to 38 healthy fetuses based on GA at the time of MRI-1. All controls had a normal structural brain MRI

study at both fetal and neonatal MRI. For the 38 PT infants at MRI-2, using Kidokoro's total abnormality score, 20 were classified as normal, 15 were mild, 1 was moderate and 2 were severe. The 3 PT infants with moderate or severe abnormality scores had grade III intraventricular hemorrhage or periventricular hemorrhagic infarction. One PT infant showed a cerebellar punctate injury on MRI-2 only, and had a score of 1 for signal abnormality in the cerebellum. Detailed clinical and demographic characteristics are presented in Table 1.

3.2. Regional cerebellar volume comparisons between PT infants and healthy fetuses

When comparing cerebellar regions between PT infants and healthy fetuses at MRI-1 and controlling only for GA at MRI, left and right cerebellar hemispheres were smaller in the PT infant versus healthy fetuses (p < .001). When we also controlled for TBV, the difference in both hemispheres held, while larger anterior-, neo- and posterior vermis volumes in the PT infants were detected compared to healthy controls (p < .001). Mean regional volumes comparisons at MRI-1 with and without controlling for TBV are presented in Tables 2a and 2b respectively.

3.3. Regional cerebellar volume comparisons between PT infants at TEA and healthy newborn

At MRI-2, PT infants continued to show decreased hemispheric volumes bilaterally and increased regional vermis volumes when controlling for GA and respective regional volumes at MRI-1. However, when we also controlled for TBV, the hemispheric differences declined and were no longer statistically significant. However, anterior-, neo- and posterior vermis remained larger in the PT infants (p < .001). Mean regional volumes comparisons at MRI-2 with and without controlling for TBV are presented in Tables 3a and 3b, respectively.

3.4. Risk factors in preterm infants associated with regional cerebellar volumetric differences

Associations between PT and clinical risk factors were examined for the anterior-, neo- and posterior vermis as these regions continued to demonstrate statistically significant differences at MRI-2. Controlling for birth weight and total brain volume, only the neovermis volume demonstrated statistically significant negative associations with

Table 1
Clinical characteristics of the cohort (N = 76).

	Term (n = 38)	Preterm (n = 38)
	Mean ± SD/Median [range]	Mean ± SD/Median [range]
Neonatal		
GA at birth (weeks)**	39.4 ± 0.9	27.5 ± 2.4
Birth weight (grams)**	3309 ± 350	978 ± 302
Female n (%)	17 (44.7)	25 (65.8)
Intubation at birth	0 (0)	26 (68.4)
Apgar score 1 min**/5 min**	8 [4–9]/9 [9–9]	5 [1–9]/8 [4–9]
Patent ductus arteriosus ligation n (%)	NA	6 (15.8)
Surgery for necrotizing enterocolitis n (%)	NA	3 (7.9)
Neonatal infection n (%)	NA	11 (31.4)
Postnatal steroids n (%)	NA	13 (34.2)
Postnatal hypertensor n (%)	NA	15 (39.5)
Postnatal sedation n (%)	NA	16 (42.1)
Days on mechanical ventilation	NA	3 [0–124]
Days on supplementary oxygen	NA	48 [2–142]
Chronic lung disease n (%)	NA	13 (34.2)
Days in NICU	NA	82 [32–142]
First MRI		
Gestational age at MRI-1 (weeks)	34.2 ± 2.0	34.3 ± 2.0
Day of life at MRI-1	NA	46 [10–91]
Second MRI		
Gestational age at MRI-2* (weeks)	41.4 ± 1.6	40.5 ± 1.7
Day of life at MRI-2**	12 [3–43]	94 [51–135]
Supratentorial injury score	NA	3 [0−11]
Total brain injury score	NA	3 [0−12]

* p < .05.
** p < .001.

birthweight, male gender and our supratentorial injury score. This predictive model accounted for 60% of the variance in volume (p < .001) and is presented in Table 4. No other risk factors were found to be associated with the anterior or posterior vermis.

4. Discussion

This study reports the first gestational-age matched comparative study of global and regional longitudinal 3-D MRI measurements of cerebellar growth between ex-utero PT infants and in-utero healthy

Table 2a
MRI-1 volume comparisons controlling for GA at MRI-1 only.

	Term Infants				Preterm Infants				Difference
Region	Mean	SE	95% CI		Mean	SE	95% CI		P-value
L_hemi	5.47	0.20	5.07	5.87	4.36	0.20	3.95	4.77	< 0.001
R_hemi	5.54	0.19	5.15	5.93	4.44	0.21	4.02	4.86	< 0.001
Ant_vermis	0.40	0.06	0.28	0.52	0.38	0.06	0.26	0.50	0.685
Neo_vermis	0.37	0.06	0.25	0.50	0.28	0.06	0.16	0.40	0.065
Post_vermis	0.26	0.06	0.14	0.39	0.27	0.06	0.16	0.38	0.849
TCV	12.02	0.37	11.28	12.80	9.73	0.39	8.94	10.53	< 0.001

L_hemi, left hemisphere; R_hemi, right hemisphere; SE, standard error; TCV, total cerebellar volume.

Table 2b
MRI-1volume comparisons controlling for GA at MRI-1 and Total Brain Volume.

	Term Infants				Preterm Infants				Difference
Regions	Mean	SE	95% CI		Mean	SE	95% CI		P-value
R_hemi	5.36	0.19	4.98	5.73	4.62	0.17	4.29	4.96	< 0.001
L_hemi	5.29	0.19	4.90	5.68	4.54	0.16	4.22	4.87	< 0.001
Ant_vermis	0.22	0.07	0.08	0.35	0.56	0.08	0.40	0.72	< 0.001
Neo_vermis	0.19	0.07	0.05	0.34	0.46	0.08	0.29	0.63	0.001
Post_vermis	0.08	0.07	−0.07	0.23	0.45	0.08	0.29	0.61	< 0.001
TCV	11.14	0.36	10.40	11.87	10.64	0.23	10.18	11.10	0.21

L_hemi, left hemisphere; R_hemi, right hemisphere; TCV, total cerebellar volume.

Table 3a
MRI-2 volume comparisons controlling for regional volume at MRI-1 and GA at MRI-2.

	Term Infants				Preterm Infants				Difference
Region	Mean	se	95% CI		Mean	se	95% CI		P-value
R_hemi	9.32	0.42	8.46	10.18	8.43	0.42	7.58	9.27	0.023
L_hemi	9.30	0.44	8.41	10.19	8.32	0.42	7.47	9.16	0.011
Ant_vermis	1.06	0.22	0.62	1.50	1.41	0.21	0.99	1.82	0.001
Neo_vermis	0.90	0.22	0.46	1.35	1.29	0.22	0.85	1.74	< 0.001
Post_vermis	0.94	0.23	0.47	1.42	1.26	0.22	0.82	1.70	0.003
TCV	21.86	0.38	21.09	22.63	20.36	0.59	19.15	21.56	0.035

L_hemi, left hemisphere; R_hemi, right hemisphere; SE, standard error; TCV, total cerebellar volume.

Table 3b
MRI-2 volume comparisons controlling for regional volume at MRI-1, GA at MRI-2 and total brain volume.

	Term Infants				Preterm Infants				Difference
Region	Mean	SE	95% CI		Mean	SE	95% CI		P-value
R_hemi	9.27	0.40	8.46	10.08	8.69	0.38	7.91	9.47	0.130
L_hemi	9.25	0.41	8.42	10.09	8.58	0.38	7.81	9.35	0.071
Ant_vermis	0.81	0.22	0.36	1.26	1.51	0.21	1.10	1.93	< 0.001
Neo_vermis	0.65	0.22	0.20	1.10	1.39	0.22	0.95	1.84	< 0.001
Post_vermis	0.69	0.24	0.21	1.17	1.36	0.22	0.92	1.80	< 0.001
TCV	20.77	0.41	19.94	21.61	21.44	0.48	20.48	22.41	0.340

L_hemi, left hemisphere; R_hemi, right hemisphere; SE, standard error; TCV, total cerebellar volume.

Table 4
Factors associated with volume differences at MRI-2 in preterm infants.

Significant region	Factors	Coeff.	SE	95% CI		p-Value
Neo Vermis	GA at MRI-2	0.0550	0.0144	0.0256	0.0843	0.001
	TBV	0.0006	0.0005	0.0005	0.0017	0.259
	Sex	−0.0876	0.0405	−0.1703	−0.0049	0.039
	Birthweight	−0.0002	0.0001	−0.0004	−0.0001	0.013
	SPI score	−0.0226	0.0078	−0.3843	−0.0068	0.007

Coeff., coefficient; SE, standard error; TBV, Total brain volume.

fetuses. Using volumetric MRI, we demonstrate regional and temporal volumetric differences in cerebellar growth in ex-utero PT infants compared with healthy in-utero fetal controls. We also demonstrate that the neovermis volume was inversely related to birthweight, male gender and supratentorial injury. These data suggest altered ex-utero cerebellar developmental programming in the absence of cerebellar parenchymal injury evident on conventional MRI.

Between 24 and 40 weeks of gestation, the cerebellum undergoes an exuberant period of growth (Volpe, 2009). Since infants as premature as 23–24 weeks gestation now commonly survive, these critical phases of cerebellar development occur in the artificially-supported extra-uterine environment of neonatal intensive care. It is likely that the hazards of premature extra-uterine life are capable of disrupting the highly regulated program of normal cerebellar development (Limperopoulos et al., 2005a; Limperopoulos et al., 2005b). Until now, inferences about 3rd trimester cerebellar growth in preterm infants have compared MRI measures to full-term healthy newborns at term equivalent age (TEA). The recent successful application of fetal brain MRI and available in-utero comparable gestational age (GA) normative fetal MRI studies by our group (Bouyssi-Kobar et al., 2016) and others are enabling us to begin to establish and compare departures from normal 3rd trimester ex-utero cerebellar development.

We report decreased cerebellar hemispheric volumes and increased anterior, neo- and posterior vermian regional volumes in the PT infants when compared to healthy fetuses at MRI-1. This early baseline (i.e. MRI-1) cerebellar hemispheric volumetric reduction was no longer

evident at the second MRI when PT infants at TEA were compared to the healthy in-utero fetuses that were imaged shortly after birth. The lack of cerebellar hemispheric volumetric differences at TEA is in keeping with several previous studies that compared PT infants at TEA to term-born control neonates using comparable 3D volumetric MRI data for total cerebellar measurements (Parikh et al., 2013) or 2D cerebral ultrasound measurements (Graca et al., 2013; Sancak et al., 2016). Our data suggest that cerebellar hemispheric growth is accelerated at TEA as recently described by Kim and colleagues (Kim et al., 2016). Ongoing longitudinal MRI studies that extend beyond term equivalent age are needed to confirm these intriguing preliminary findings.

Our data also showed no differences in volumetric growth in all three regional vermian measurements (i.e. anterior, neo and posterior) at our two measurement time-points which is also in accordance with Kim et al.'s study that reported a slower growth rate in the vermis before TEA age (Kim et al., 2016). However, to our knowledge our study is the first to describe persistent vermian overgrowth in PT infants when compared to healthy controls evaluated both during the fetal period and postnatal period. Notably, we did not find any other 3D volumetric reports that compared the cerebellar regional growth in PT infants between birth and term equivalent age, thus limiting any comparisons to existing literature. We did however identify two studies reporting a larger cerebellar vermis, as assessed by 2D measurements of cranial ultrasound in PT infants at TEA when compared to full term infants (Graca et al., 2013; Sancak et al., 2016). Nevertheless, unlike our study, these differences were not statistically significant when accounting for infant head size. Taken together, our findings suggest that unlike the cerebellar hemispheres, the vermian volumetric alterations observed soon after preterm birth persist at TEA. This regional alteration in the development of the vermis may represent a selective vulnerability to decreased apoptosis of the cerebellar vermis following early extra-uterine exposure over the third trimester. We previously reported reduced mean diffusivity in the cerebellar vermis (Brossard-Racine et al., 2017a) and increased cerebellar choline (Brossard-Racine et al., 2017b) in PT infants at TEA when compared to healthy controls. We postulated that these microstructural and biochemical disturbances represent an increase in cellular density that could be a consequence of failed

apoptosis, as hypothesized in other neurodevelopmental disorders such as fetal ventriculomegaly (Kyriakopoulou et al., 2014), postnatal hydrocephalus (Benvenisti et al., 2015), and autism (Courchesne, 2002; Courchesne, 2004). To date, available evidence points to arrested cerebellar growth, especially in the presence of parenchymal injuries (Kim et al., 2016; Tam et al., 2009; Limperopoulos et al., 2005c). The results of the current study suggest that the preprogrammed cerebellar developmental course is complex and topographically distinct with areas of regional overgrowth. The extent to which regional cerebellar overgrowth may represent cerebellar maldevelopment is unclear and awaits further study.

Although we observed similar growth patterns in the anterior, neo and posterior vermis, our exploratory risk factors analysis revealed different associations across these three vermian regions. Interestingly, in our PT group, only the growth of the neovermis showed a negative association with male gender, birthweight and supratentorial brain injury severity. Kim et al.'s study also demonstrates an association between birthweight, supratentorial injury and hindbrain growth (Kim et al., 2016). The lack of association with other common clinical risk factors that previously demonstrated associations with reduced cerebellar volume such as post-natal steroid treatment (Bouyssi-Kobar et al., 2016; Tam et al., 2011) and the use of sedation (Zwicker et al., 2016) may be due to our small sample of PT infants and/or the method we used to collect exposure to medications in this study. Details regarding dosage dependent exposure was beyond the scope of our exploratory analyses of risk factors. Future studies are therefore needed to ascertain the dosage dependent effects of medications on regional cerebellar growth. However, it is also plausible that these risk factors may selectively affect other cerebellar regions that did not show accelerated growth. The fact that we only found significant clinical risk factor relationships with the neovermis, and bearing in mind that the neo vermis forms after the posterior and inferior vermis developmentally, could reflect an increased regional vulnerability (Wang and Zoghbi, 2001). We and others have previously reported a prevalent and striking neuropsychological phenotype, that we term the developmental cerebellar cognitive affective syndrome (Brossard-Racine et al., 2015). Considering the high prevalence of neurodevelopmental disorders in the PT population (Jarjour, 2015; Milner et al., 2015), and the robust associations between vermian alterations and many neurodevelopmental disorders including autism spectrum disorders (Stoodley, 2014; Hampson and Blatt, 2015), we believe that our preliminary findings will serve as hypothesis generating for future investigations into the role of altered vermian development and neurodevelopmental disabilities in PT survivors.

The functional topography of the mature cerebellum is based on its widespread anatomical connections with the cerebral cortex, where different regions within the cerebellum at a hemispheric, and lobular level mediate motor, cognitive, language, and social-affective functions (Stoodley and Schmahmann, 2009; Stoodley and Limperopoulos, 2016). To date, the emerging functional topography of the immature cerebellum has not been studied. Our studies report regional alterations of the developing cerebellum that could interfere with the optimal development of behavior and cognition (Stoodley and Limperopoulos, 2016). Ongoing studies are needed to better elucidate the role of regional alterations in cerebellar development on long-term neurodevelopmental outcome.

Our study limitations deserve mention. Manual parcellations of the cerebellum were performed by two independent evaluators which could have introduced its share of bias. However, we demonstrated very high intra-rater and inter-rater reliability with our parcellation technique, which minimized any evaluator bias. Moreover, the high-water content in fetal and neonatal brains and low contrast provided by 1.5 and 3 Tesla MRI scanners prevent us from applying most automatic segmentation and parcellation pipelines validated in the adult brain. We therefore believe that manual parcellation was the best approach for these very challenging data. Another important limitation to consider is

the variability in GA between subjects at both MRIs. Nevertheless, our matched design between PT infants and in-utero fetuses and our precise statistical modeling has accounted for this variability. Lastly, our modest sample size may have limited our ability to detect effects and associations of smaller magnitude and consequently our findings mandate cautious interpretation.

5. Conclusion

We show for the first time that regional cerebellar vermian growth is altered following PT birth in the absence of demonstrable cerebellar parenchymal injury on conventional MRI. Longitudinal follow-up of this cohort will provide insights into the long-term impact of altered vermian growth on neurodevelopmental outcome of PT infants.

References

Barkovich, A., 2005. Pediatric neuroimaging, 4th ed. Williams & Wilkins, Philadelphie, PA.

Benvenisti, H., et al., 2015. "Growing" cerebellum in an infant after shunt insertion. Pediatr. Neurol. 52 (2), 222–225.

Bogovic, J.A., et al., 2013. Approaching expert results using a hierarchical cerebellum parcellation protocol for multiple inexpert human raters. NeuroImage 64, 616–629.

Bouyssi-Kobar, M., et al., 2016. Third trimester brain growth in preterm infants compared with in utero healthy fetuses. Pediatrics 138(5).

Brossard-Racine, M., et al., 2014. Prevalence and spectrum of in utero structural brain abnormalities in fetuses with complex congenital heart disease. AJNR 35 (8), 1593–1599.

Brossard-Racine, M., du Plessis, A.J., Limperopoulos, C., 2015. Developmental cerebellar cognitive affective syndrome in ex-preterm survivors following cerebellar injury. Cerebellum 14 (2), 151–164.

Brossard-Racine, M., et al., 2017a. Cerebellar microstructural organization is impeded by complications of premature birth: a case-control study. J. Pediatr. 182, 28–33.

Brossard-Racine, M., et al., 2017b. Altered cerebellar biochemical profiles in infants born prematurely. Sci. Rep. 7 (1), 8143.

Cho, K.H., et al., 2011. Early fetal development of the human cerebellum. Surg. Radiol. Anat. 33 (5), 523–530.

Courchesne, E., 2002. Abnormal early brain development in autism. Mol. Psychiatry 7 (Suppl. 2), S21–S23.

Courchesne, E., 2004. Brain development in autism: early overgrowth followed by premature arrest of growth. Ment. Retard. Dev. Disabil. Res. Rev. 10 (2), 106–111.

Gholipour, A., et al., 2011. Fetal brain volumetry through MRI volumetric reconstruction and segmentation. Int. J. Comput. Assist. Radiol. Surg. 6 (3), 329–339.

Graca, A.M., et al., 2013. Preterm cerebellum at term age: ultrasound measurements are not different from infants born at term. Pediatr. Res. 74 (6), 698–704.

Hampson, D.R., Blatt, G.J., 2015. Autism spectrum disorders and neuropathology of the cerebellum. Front. Neurosci. 9, 420.

Jarjour, I.T., 2015. Neurodevelopmental outcome after extreme prematurity: a review of the literature. Pediatr. Neurol. 52 (2), 143–152.

Kidokoro, H., Neil, J.J., Inder, T.E., 2013. New MR imaging assessment tool to define brain abnormalities in very preterm infants at term. AJNR Am. J. Neuroradiol. 34 (11), 2208–2214.

de Kieviet, J.F., et al., 2012. Brain development of very preterm and very low-birthweight children in childhood and adolescence: a meta-analysis. Dev. Med. Child Neurol. 54 (4), 313–323.

Kim, H., et al., 2016. Hindbrain regional growth in preterm newborns and its impairment in relation to brain injury. Hum. Brain Mapp. 37 (2), 678–688.

Kyriakopoulou, V., et al., 2014. Cortical overgrowth in fetuses with isolated ventriculomegaly. Cereb. Cortex 24 (8), 2141–2150.

Limperopoulos, C., et al., 2005a. Late gestation cerebellar growth is rapid and impeded by premature birth. Pediatrics 115 (3), 688–695.

Limperopoulos, C., et al., 2005b. Cerebellar hemorrhage in the preterm infant: ultrasonographic findings and risk factors. Pediatrics 116 (3), 717–724.

Limperopoulos, C., et al., 2005c. Impaired trophic interactions between the cerebellum and the cerebrum among preterm infants. Pediatrics 116 (4), 844–850.

Limperopoulos, C., et al., 2007. Does cerebellar injury in premature infants contribute to the high prevalence of long-term cognitive, learning, and behavioral disability in survivors? Pediatrics 120 (3), 584–593.

Milner, K.M., et al., 2015. Long-term neurodevelopmental outcome in high-risk newborns in resource-limited settings: a systematic review of the literature. Paediatr. Int. Child Health 35 (3), 227–242 p. 2046905515y0000000043.

Parikh, N.A., et al., 2013. Perinatal factors and regional brain volume abnormalities at term in a cohort of extremely low birth weight infants. PLoS One 8 (5), e62804.

Sancak, S., et al., 2016. Effect of prematurity on cerebellar growth. J. Child Neurol. 31 (2), 138–144.

Smith, S.M., 2002. Fast robust automated brain extraction. Hum. Brain Mapp. 17 (3), 143–155.

StataCorp, 2015. Stata Statistical Software: Release 14, ed. C. Station. StataCorp LP, TX.

Stoodley, C.J., 2014. Distinct regions of the cerebellum show gray matter decreases in autism, ADHD, and developmental dyslexia. Front. Syst. Neurosci. 8, 92.

Stoodley, C.J., Limperopoulos, C., 2016. Structure-function relationships in the developing cerebellum: evidence from early-life cerebellar injury and neurodevelopmental disorders. Semin. Fetal Neonatal Med. 21 (5), 356–364.

Stoodley, C.J., Schmahmann, J.D., 2009. Functional topography in the human cerebellum: a meta-analysis of neuroimaging studies. NeuroImage 44 (2), 489–501.

Tam, E.W., et al., 2009. Cerebellar development in the preterm neonate: effect of supratentorial brain injury. Pediatr. Res. 66, 102–106.

Tam, E.W., et al., 2011. Preterm cerebellar growth impairment after postnatal exposure to glucocorticoids. Sci. Transl. Med. 3 (105), 105ra105.

Tustison, N.J., et al., 2010. N4ITK: improved N3 bias correction. IEEE Trans. Med. Imaging 29 (6), 1310–1320.

Volpe, J.J., 2009. Cerebellum of the premature infant: rapidly developing, vulnerable, clinically important. J. Child Neurol. 24 (9), 1085–1104.

Wang, V.Y., Zoghbi, H.Y., 2001. Genetic regulation of cerebellar development. Nat. Rev. Neurosci. 2 (7), 484–491.

Yushkevich, P.A., et al., 2006. User-guided 3D active contour segmentation of anatomical structures: significantly improved efficiency and reliability. NeuroImage 31 (3), 1116–1128.

Zwicker, J.G., et al., 2016. Smaller cerebellar growth and poorer neurodevelopmental outcomes in very preterm infants exposed to neonatal morphine. J. Pediatr. 172, 81–87.